CHEMISTRY
A EUROPEAN JOURNAL

DOI: 10.1002/chem.200700455

Probing Hydroxyl Radicals and Their Imaging in Living Cells by Use of FAM–DNA–Au Nanoparticles

Bo Tang,*[a] Ning Zhang,[a] Zhenzhen Chen,[a] Kehua Xu,[a] Linhai Zhuo,[a] Liguo An,[b] and Guiwen Yang[b]

Abstract: The incorporation of gold nanoparticles (Au NPs) as quencher modules in fluorescent probes for DNA damage caused by intracellular hydroxyl radicals (HO•) is reported. Au NPs of 15 nm diameter were decorated with DNA oligomers terminating in thiol functions in their 3′ positions and possessing 5′ fluorophore modifications. The Au NPs, which have high extinction coefficients, functioned as excellent fluorescent quenchers in the fluorophore–Au NP composites. FRET is switched off as a factor of HO•-induced strand breakage in the single-stranded DNAs, restoring the fluorescence of the quenched fluorophores, which can be followed by spectrofluorimetry. In vitro assays with HO•-generating Fenton reagent demonstrated increases in fluorescence intensity with a linear range from 8.0 nM to 1.0 μM and a detection limit as low as 2.4 nM. Confocal microscopic imaging of macrophages and HepG2 revealed that the probe is cell-permeable and intracellular HO•-responsive. The unique combination of good selectivity and high sensitivity establishes the potential value of the probe for facilitating investigations of HO•-mediated cellular homeostasis and injury.

Keywords: FRET (fluorescence resonant energy transfer) · hydroxyl radicals · living cells · nanoparticles

Introduction

Currently, the biochemistry of oxygen activation and the biological significance of reactive oxygen species (ROS) are attracting much interest. Oxygen-centered free radicals—such as singlet oxygen, superoxide anion radical, hydrogen peroxide, hydroxyl radical, and peroxynitrite—are potent agents responsible for many potentially pathological effects and aging.[1–3] The OH radical, one of the strongest oxidants known, is primarily responsible for cellular disorders and cytotoxic effects that can be traced back to oxidative damage to DNA,[4] proteins,[5] or lipids.[6] However, more detailed understanding of the importance of HO• in initiating cellular injury has seldom been achieved, due largely to a lack of highly selective, sensitive, and quantitative methods for its detection under the complicated oxidative circumstances found in biological systems.

Several methods to detect ROS, including electron spin resonance[7] and chemiluminescence,[8] have been developed, but fluorescence detection is superior in terms of high sensitivity and of making ROS "visible" in living cells.[9–12] Centrally to its use, fluorescent probes have evolved into an extremely powerful tool for evaluating the characteristics of HO•-related biological processes.[13] These probes include the succinimidyl ester of coumarin-3-carboxylic acid (SECCA),[14] fluorescamine-derivatized nitroxide,[15] and chromophores with ROS-cleavable protecting groups.[16,17] However, limitations of currently available HO•-responsive probes include interference from background fluorescence from other ROS and lack of effective direct means of biological monitoring. As Hempel and co-workers have pointed out, the most commonly used fluorophore for cellular ROS detection—2′,7′-dichlorodihydrofluorescein (DCFH)—lacks specificity between ROS and suffers from autoxidation; that is, the fluorescence increases even in the absence of ROS upon continued exposure to light irradiation.[18] Hence, the design of selective and stable fluorescent probes for individual ROS species and assays based on fluorescence imaging

[a] Prof. B. Tang, Dr. N. Zhang, Z. Chen, K. Xu, L. Zhuo
College of Chemistry
Chemical Engineering and Materials Science
Engineering Research Center of Pesticide and Medicine
Intermediate Clean Production, Ministry of Education
Shandong Normal University, Jinan 250014 (China)
Fax: (+86) 531-8618-0017
E-mail: tangb@sdnu.edu.cn

[b] Prof. L. An, G. Yang
College of Life Science, Shandong Normal University
Jinan 250014 (China)

WILEY InterScience DISCOVER SOMETHING GREAT
© 2008 Wiley-VCH Verlag GmbH & Co. KGaA, Weinheim

allowing for the assessment of single ROS generated from living cells would be of special interest for biochemistry.

Recent advances in the growing field of nanobiotechnology have resulted in favorable participation by inorganic nanoparticles in FRET-based (fluorescence resonance energy transfer-based) studies, due to their size-dependent physical and chemical characteristics.[19–22] Au NPs, which display extremely high quenching efficiencies, open up new perspectives in the use of hybrid materials as sensitive probes in fluorescence-based assays.[23,24] Since Mirkin[25] and Alivisatos[26] made the important step of exploiting the linking of Au NPs to one another through complementary DNA strands, many fascinating ideas for applications of DNA-based nanostructures have been developed.[27–30] To the best of our knowledge, however, no attempt to employ DNA-conjugated fluorophore–Au NP composites for monitoring of ROS in living cells has previously been made. Our strategy here has been to design a new type of fluorescent probe—FAM–DNA–Au NPs—for trapping HO•, the detection mechanism being based the switching off of FRET through the highly selective HO•-induced cleavage of DNA strands. In vitro assays with HO•-generating Fenton reagent demonstrate an increase in fluorescence intensity attributable to HO•-induced DNA strand breakage. The probe has the merits of a very low background signal and hence high achievable sensitivity, coupled with excellent selectivity toward HO• over competing ROS. Confocal microscopy studies of macrophages and HepG2 have revealed that the probe is cell-permeable and intracellular HO•-responsive. In particular, the presence of Au NPs featuring broad absorption in the UV and visible light regions provides efficient background removal to avoid interference from autofluorescence. The features of these particular spectral regions make them ideal for using the probe to detect HO• in living cells. Our results have established the value of this nanotechnology-based probe for imaging of HO• in living cells and open a new window to facilitate investigations of ROS-mediated cell behavior.

Results and Discussion

Designing FAM–DNA–Au NPs for HO•: The available evidence indicates that HO• radicals produced in vivo from H_2O_2 by a metal-mediated reaction may attack and cleave the DNA phosphate/deoxyribose backbone in a largely sequence-independent manner.[31,32] Oxidative attack by HO• on the deoxyribose moiety leads to the release of free bases from DNA, generating strand breaks with various sugar modifications and abasic (AP) sites (sites where a DNA base has been lost).[33] Cleavage by HO• occurs not only in DNA but also in protein. However, this does not interfere with probe specificity for HO•, since DNA is cleaved much more efficiently than protein, due to its higher sensitivity toward HO•.[34] The probe system involves an artful design containing attack sites for HO• functions as outlined in Scheme 1. Single-stranded DNAs labeled with thiol groups

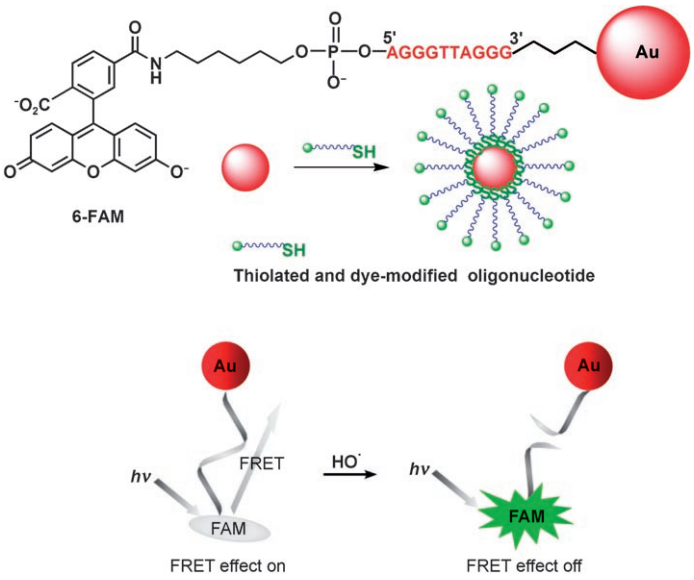

Scheme 1. Chemical structure of a FAM–DNA–Au NP and schematic illustration of its FRET-based operating principles.

at their 3′-termini and 6-carboxyfluorescein (6-FAM; $\lambda_{ex}=490$ nm, $\lambda_{em}=517$ nm) at their 5′-termini are attached to a 15 nm Au NP acting as a nano-quencher unit. FAM remains a reagent of choice for the preparation of hydrolytically stable fluorescent DNA conjugates. When HO• breaks the DNA strands and the FAM is divorced from the particle surface, the FAM fluorescence originally quenched by the Au NPs will be recovered, and the fluorescence increase will be related to the HO• concentration, thus providing a new assay of HO• in biological systems.

Stern–Volmer Plot: The absorption spectrum of Au NPs overlaps the emission spectrum of FAM, and so efficient FRET between the donor–acceptor pair should be expected.[35] Indeed, when the concentration of FAM was stabilized at 0.3 μM, while the Au NP content was varied from 0–1.2 nM in increments of 0.2 nM, a regular decrease in the emission of FAM was observed. Fluorescence quenching is described by the well known Stern–Volmer equation:[36]

$$F_0/F = 1+K_{SV}[\text{Au NPs}]$$

where F_0 and F denote the steady-state fluorescence intensities in the absence and in the presence, respectively, of quencher Au NPs. A plot of F_0/F versus [Au NPs] produced a straight line as shown in Figure 1, the slope of which gave the Stern–Volmer constant ($K_{SV}=1.54\times10^9\,\text{M}^{-1}$); knowing the lifetime of the donor FAM ($\tau_0=4.5$ ns), we were then able to estimate its quenching rate constant: $k=K_{SV}/\tau_0=3.4\times10^{17}\,\text{M}^{-1}\,\text{s}^{-1}$.

Performance characteristics and statistical analysis: We monitored changes in the fluorescence spectra of FAM–DNA–Au NPs in the presence of different concentrations of

 © 2008 Wiley-VCH Verlag GmbH & Co. KGaA, Weinheim

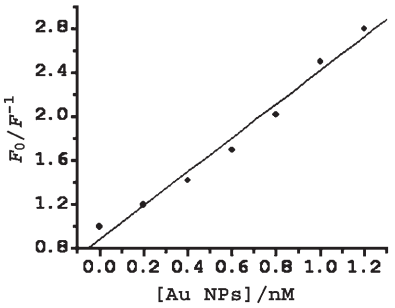

Figure 1. Stern–Volmer plot of F_0/F versus [Au NPs]. The linear approximation gives $F_0/F = 0.88 + 1.54$ [Au NPs], $R = 0.9905$.

HO• as shown in Figure 2. As expected, there was near-zero background fluorescence before addition of HO•, with a donor quenching efficiency close to 100%. Upon the occurrence of HO•-induced DNA chain scission, however, the constrained conformation was opened, and the release of the cleaved fragment resulted in a distinct fluorescence increase due to the elimination of the FRET effect. The change in the fluorescence intensity relative to that of the probe increased with increasing concentration of Fenton reagent. At concentration ranges higher than 10 μM the fluorescence intensity was saturated, indicating that nearly all of the probe in the sample solution had reacted with HO• and that all of the linkers of the probe had been cleaved.

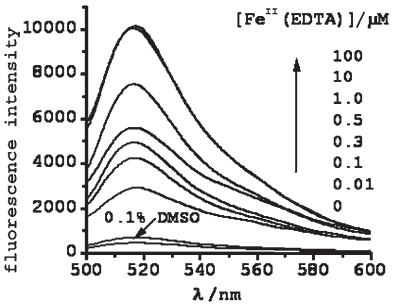

Figure 2. Fluorescence spectra of 1× probe solutions (250 μL, 0.3 M PBS, pH 7.4) after addition of varying amounts of Fenton reagent (Fe^{II}-(EDTA)/H_2O_2 1:6 mol mol^{-1}). All spectra were obtained after incubation at 37 °C for an equilibration period of 15 min.

To confirm further that the increase in fluorescence emission was indeed due to the HO•-induced breakdown of DNA chains, DMSO, a typical HO•-scavenger,[37] was used. Before the addition of Fenton reagent to trigger the reaction, DMSO was introduced into the reaction mixture, and the extent of fluorescence increase was greatly suppressed.

Furthermore, we also examined the relationship between the concentration of Fe^{II}(EDTA) in the added Fenton reagent and the fluorescence increase in the Fenton reaction. As can be seen from the calibration curve of fluorescence signals versus Fe^{II}(EDTA) concentrations shown in Figure 3, the fluorescence increase is proportional to the concentration of Fe^{II}(EDTA) in the 8.0 nM–1.0 μM range. Fe^{II}(EDTA) has often been used as an effective inorganic reagent for mediating HO• production from H_2O_2 according to the Fenton reaction equation.[38] A concentration of Fe^{II}(EDTA) as low as 2.4 nM, generating approximately the expected quantity of HO•, could readily be detected. The precision, expressed as the relative standard deviation (% RSD), obtained from a series of 11 standards each containing 1 μM of HO•, was 2.7. Therefore, the probe can detect HO• formed in the Fenton reaction in the form of a dose-dependent increase in fluorescence.

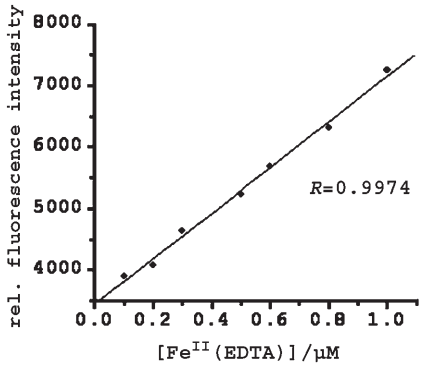

Figure 3. Linear plot of fluorescence intensity as a function of HO• concentration.

Amount of alkanethiol-oligonucleotides loaded on Au NPs: In previous work by Pär Sandström,[39] alkanethiol-tagged oligonucleotides were incubated with the particles in a 200-fold excess of DNA strands. This ratio was used to ensure that each particle bound at least one oligomer molecule. Deficiency in the amount of Au NPs made DNA deposition insufficient, and high background fluorescence could be observed. Use of excess Au NPs resulted in effective quenching of the FAM fluorescence, but only very limited fluorescence recovery would be observed despite HO•-induced strand breakage. By chemically tailoring the density of alkanethiol-oligonucleotides bound to the surface of Au NPs, we found that 300-fold molar excesses of DNA strands may be the appropriate amount regarding our experimental conditions for HO• determination.

Specifically thiol-modified oligonucleotides tend to be anchored to the particle at one end and thus stand up from the surface. The loading of particles with DNA achieved by this method was estimated by a fluorescence-based method.[40] Dithiothreitol at 1.7 mM concentration was used to displace the surface-bound oligonucleotides rapidly through an exchange reaction, and the amount of released DNA was measured by fluorescence. Standard curves were derived according to the known concentrations of FAM-labeled oligonucleotides under identical conditions (such as buffer pH, salt and dithiothreitol concentrations). The fluorescence signals were converted into molar concentrations of the thiol-modified oligonucleotides by interpolation from a standard linear calibration curve. By dividing the total number of oligomer molecules by the original Au NPs con-

 © 2008 Wiley-VCH Verlag GmbH & Co. KGaA, Weinheim

centration, we calculated that there were 144 oligomers per Au NP.

Conditions of metal-mediated Fenton reaction: It is generally assumed[38,41] that HO• is generated in biological processes from H_2O_2 through the Fenton reaction, known from inorganic chemistry. Metal binding can occur on DNA, and this can lead to partial site-specificity in HO• formation. Fe complexed to chromatin functions as a catalyst for the Fenton reaction in vivo, similarly to the role played by Fe-chelate in vitro. Fe commonly catalyzes the decomposition of H_2O_2 to produce HO•, and an even higher number of strand breaks is observed when Fe is complexed with EDTA, consistently with the well known participation of Fe-EDTA chelate in the Fenton reaction.[42]

The kinetic behavior of the reaction was investigated (Figure 4) with the aim of determining the optimal experimental conditions for the proposed method. The fluorescence signal was recorded as a function of reaction time on addition of Fe^{II}(EDTA) at 1 μM concentration to stimulate the reaction. The fluorescence signal increased sharply up to the 15 min time point and then remained almost constant with increasing reaction time. At 10 nM Fe^{II}(EDTA) concentration, however, the kinetics of HO• production and DNA damage were fast enough to be finished within 10 min. Therefore, a 15 min reaction time can be selected in subsequent experiments.

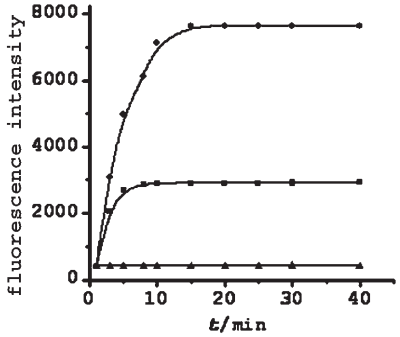

Figure 4. Fluorescence intensity of the system was recorded as a function of reaction time after the introduction of Fenton reagent into 1× probe buffer solutions (250 μL, 0.3 M PBS, pH 7.4) at 37 °C. ▲: Blank. ■: [Fe^{II}-(EDTA)]/[H_2O_2], 10 nM:60 nM. ◆: [Fe^{II}(EDTA)]/[H_2O_2], 1 μM:6 μM.

Effects of various species on the probe: Perhaps the most attractive feature of the approach is its selectivity for HO•, especially in cellular systems, and so the effects of interfering species normally found in association with HO• were studied (Figure 5). The experimental results demonstrated that the probe showed no remarkable fluorescence output when various ROS or reductants—such as superoxide anion radical ($O_2^{\bullet-}$), hydrogen peroxide (H_2O_2), hypochlorite ($ClO^{\bullet-}$), peroxynitrite ($ONOO^-$), single oxygen ($^1O_2$), nitric oxide (NO), glutathione (GSH), and 1,4-hydroquinone (HQ)—were added with an equal amount of HO• (final 1 μM for each). However, it appears that addition of $ONOO^-$ resulted in a relatively large fluorescent augmentation. This is thought to be because peroxynitrous acid decomposes to give about 28% free HO•, so one would expect a relatively stronger response of the probe if it is indeed specific for HO•. A slight fluorescence yield from added Fe^{II} in the absence of H_2O_2 might further account for the probe specificity.

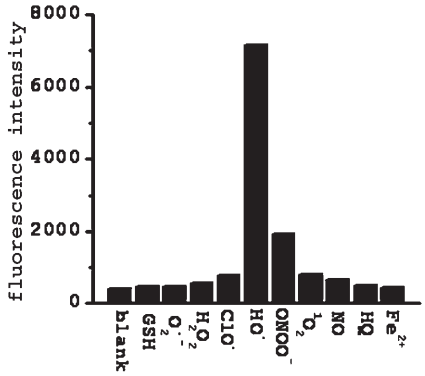

Figure 5. Comparison of the fluorescent responses of probe to various ROS and reductants. The fluorescence intensities of the system were recorded after the introduction of various ROS and reductants (final 1 μM for each) into 1× probe buffer solutions (250 μL, 0.3 M PBS, pH 7.4). All data were obtained after incubation at 37 °C for an equilibration period of 15 min. $*O_2^{\bullet-}$ was created by the enzymatic reaction of XA/XO, and $^1O_2$ was obtained by addition of NaClO to H_2O_2 (10:1 mol per mol). $ONOO^-$ and NO were delivered by use of 3-morpholinosydnonimine (SIN-1), and 3-(aminopropyl)-1-hydroxy-3-isopropyl-2-oxo-1-triazene (NOC-5), respectively.

Imaging of intracelluar HO•: Most probes rely on their positively charged surfaces to ensure cellular uptake. Unexpectedly, FAM–DNA–Au NPs readily entered cells despite their coating with negatively charged DNA.[43] We performed uptake experiments with different cell types, including mouse peritoneal macrophages and HepG2 (cancerous liver cells). Probe-loaded macrophages showed weak intracellular background fluorescence (Figure 6a). A strong fluorescence signal was observed upon stimulation of probe-loaded macrophages with phorbol myristate acetate (PMA, a stimulator of cell respiratory burst to give rise to ROS) over 1 h, as determined by confocal microscopy on living cells (Figure 6b and c). Incubation of probe-loaded macrophage cells with DMSO as a HO• scavenger prior to PMA stimulation resulted in negligible fluorescence yields (Figure 6e), highlighting the specificity of the measurement. Furthermore, we provide a confocal microscopic image of HepG2 (Figure 6f) as a practical biological model to demonstrate the practicability and high membrane penetrability of the probe.

Apoptosis markers can address cell viability; acridine orange (AO) is a vital fluorescent stain useful for identifying cell apoptosis.[44] AO staining should be informative for checking putative toxic effects of the treatment with probe and confirming that the cells were viable throughout the imaging experiments. The experiment showed that cells did

 © 2008 Wiley-VCH Verlag GmbH & Co. KGaA, Weinheim

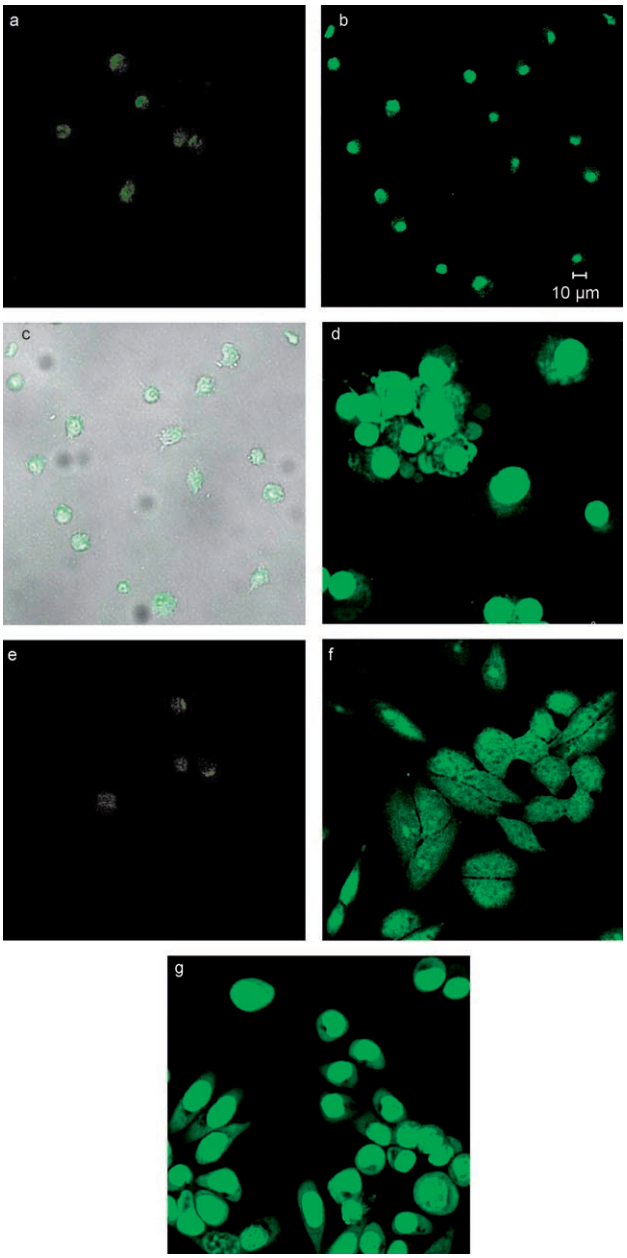

Figure 6. Confocal fluorescence and phase-contrast images of living cells. a) Fluorescence image of macrophages incubated with the probe for 30 min at 37 °C. b) Fluorescence image of probe-stained macrophages stimulated with PMA for 1 h at 37 °C. c) Brightfield image of live macrophages shown in panel b, confirming their viability. d) AO staining of probe-loaded macrophages, confirming their viability. e) Probe-loaded cells were treated with DMSO (0.1 %) for 1 h prior to PMA stimulation. f) Fluorescence image of HepG2 incubated with the probe for 30 min at 37 °C. g) AO staining of probe-loaded HepG2 cells, confirming their viability.

not display typical apoptosis features such as cell shrinkage, membrane blebbing, nucleus condensation, or the common nucleus fragmentation (Figure 6d and g). Taken together, these contrast images indicated that FAM–DNA–Au NPs, as a cell-permeable probe, can respond to changes in intracellular HO• concentrations, and that native cellular species do not contribute to the fluorescence imaging, as shown in the HO• scavenging test (Figure 6e).

Reliability assessment in cell biological applications: In order to evaluate the reliability of this method, macrophages were divided into four parallel groups. Cell imaging tests were performed under the same experimental conditions as described (Figure 6b). Average fluorescence intensities of individual cells (more than 50 cells) in each group were determined with the aid of an Image Pro plus analysis system. Average fluorescence intensities were 746, 709, 713, and 719, which demonstrated good reliability of the method in living cells.

A cell extract test was performed to evaluate the precision of the method. According to the procedure outlined above, fluorescence readings of the cell supernatant solutions were undertaken. Incubation of macrophage cells with HO• scavenger DMSO (0.1 %) for 1 h prior to probe loading resulted in autofluorescence output. The detected HO• content of PMA-stimulated cells was 0.31 μM on average, derived from the standard curve and the regression equation. The average recovery test was carried out by using the standard addition method, and the RSD obtained from a series of six cell suspensions was 3.4 %. The results given in Table 1 indicated that the recovery and precision of the method applied to determine HO• in cell extracts were satisfactory.

Table 1. Determination of HO• in cell extracts ($n=6$).

Sample	HO• content [μM]	Added [μM]	Found [μM]	Mean [μM]	Average recovery [%]	RSD [%]
Cell extracts	0.31 ± 0.04	0.30	0.58, 0.62, 0.60, 0.61, 0.59, 0.56	0.59 ± 0.02	93.3	3.4

Conclusions

What has been demonstrated here is that FAM–DNA–Au NPs could serve as a new probe for detecting HO•, contributing to shedding new light in cases of appropriately suited imaging of HO• at the cellular level. The probe features excellent selectivity for HO• over competing cellular ROS. Application of the FAM–DNA–Au NPs in macrophage assays resulted in low background signals before and significant fluorescence readouts after stimulation of cellular HO• production by PMA, and effective signals were also readily obtained in HepG2 by use of the probe. It is to be expected that this novel probe might work not only for in vivo HO• imaging, with little or no interference from autofluorescence, but might also quantify HO• in ex vivo biological systems such as cell extracts with satisfactory results. Our results have established the value of this nanotechnology-based probe for imaging of HO• in living cells and hold considerable promise in investigations of cellular behavior mediated by other biological species.

© 2008 Wiley-VCH Verlag GmbH & Co. KGaA, Weinheim

Experimental Section

Materials and physical instrumentations: Hydrogen tetrachloroaurate(III) ($HAuCl_4 \cdot 3H_2O$) and trisodium citrate were purchased from Aldrich Chemical Co. and used as supplied. HO• is chemically generated through the Fenton reaction, catalyzed by a transition metal such as Fe^{II} in a chelated state. Fe^{II}(EDTA) solution (5 mM) was prepared daily by adding the appropriate amount of ammonium ferrous sulfate to EDTA solution (Fe/EDTA 1:3 mol mol^{-1}) in Sartorius ultrapure water (18.2 MΩ cm^{-1}), giving a slightly green, clear solution. A stock solution (100 mL) of H_2O_2 (0.3 M) was freshly prepared by diluting H_2O_2 (30%, 3.4 mL) with water, and the concentration was standardized by titration with potassium permanganate. The single-stranded oligonucleotide used in this work (synthesis and purification by Shanghai Sangon, China) was derivatized with 3′-alkanethiol and 5′-FAM to give the following sequence: 5′-FAM-$(CH_2)_6$-AGGGTTAGGG-$(CH_2)_3$-SH-3′. Absorption spectra were recorded on a UV-1700 spectrophotometer (Shimadzu Corp. Kyoto, Japan). Fluorimetric spectra were measured with an Edinburgh FLS 920 spectrofluorimeter (Edinburgh Instruments Ltd., UK) fitted with a xenon lamp in a quartz cuvette (1.0 cm optical path) as the container. Spectrometer slits were set for 1.0 nm band-pass. Transmission electron microscopy (TEM) images were collected with a Hitachi Model H-800 instrument operating at 100 keV accelerating voltage.

Gold-particle fabrication: The starting step for this work was the preparation of an aqueous solution of Au NPs (15 nm). Near-monodisperse Au NPs of 15 nm diameter were prepared by the classical citrate reduction route pioneered by Frens.[45] All glassware was cleaned in aqua regia (3 parts HCl, 1 part HNO_3), rinsed with Sartorius water, and then oven-dried prior to use. Briefly, trisodium citrate (1%, 5.25 mL) was added rapidly to $HAuCl_4$ (0.01%, 150 mL) that was brought to reflux while stirring. This mixture was heated at reflux for an additional 15 min, during which the color changed to deep red. The solution was then set aside to cool to room temperature. This resulted in Au NPs with a net negative charge from the citrate ions stabilizing the particles. The size distribution and quality of the resulting particles, of average diameter 15.7 ± 2 nm, were determined by TEM. Please note that we denote the concentration of the as-prepared Au NPs to be 1 × (1.2 × 10^{15} particles L^{-1}, ≈2 nM)[46] with a high molar extinction coefficient (ε at 520 nm) 6.1 × 10^8 M^{-1} cm^{-1}. A typical solution of 15 nm diameter Au NPs was chosen because they could be readily prepared with little deviation in size (±2 nm), and with a characteristic absorption band centered at 520 nm, so that the FRET process was highly efficient as there was an appreciable overlap between the emission spectrum of the FAM donor and the absorption spectrum of the Au NP acceptor.

Attachment of fluorescent alkanethiol oligonucleotides to Au NPs: In a famous "Northwestern" preparation by Mirkin and co-workers,[47–48] fluorescent alkanethiol oligonucleotides of 10 bases corresponding to 3.4 nm were attached to Au NPs by incubation of thiolated single-stranded oligonucleotides with a gold solution (250 μL, 1×) at a 300:1 mol ratio. After standing for 16 h, the solution was gently treated with phosphate buffer (10 mM, pH 7.4) and NaCl (0.1 M), and allowed to "age" for an additional 40 h at room temperature. Please pay attention to the fact that a gradual increase in electrolyte concentration and ionic strength over the course of DNA deposition significantly increase surface coverage and consequently particle stability. Unbound oligonucleotides were then removed by repeated centrifugation and suspension of the red oily precipitate (Eppendorf 5417R Centrifuge, 14000 rpm, ×2). The DNA-complexed particles were finally redispersed in fresh PBS (250 μL, 0.3 M, pH 7.4). This procedure was used to prepare all the probes described here, and for simplicity, their concentrations have been presented as 1× (1× Au NPs and 0.6 μM fluorescent alkanethiol oligonucleotides unless otherwise noted).

The difference in the UV/Vis spectra of unmodified Au NPs of and Au NPs modified with fluorescent thiol-oligonucleotides (Figure 7) is attributed to slightly different particle size distributions, coupled with a decrease in particle concentration during the workup of the oligonucleotide-modified particles.

Fluorescence detection: A PBS buffer (0.3 M, pH 7.4) containing 1× probe solutions (250 μL) was incubated for HO• cleavage at 37 °C for an equilibration period of 15 min after addition of Fe^{II}(EDTA) (10 nM–100 μM) and H_2O_2 (60 nM ≈ 600 μM). Each sample solution was diluted with pure PBS buffer to a final volume of 500 μL, and a fluorescence spectrum of the diluted sample solution was obtained. Care was taken to keep the pH and ionic strength of the sample solutions the same for all measurements, due to the sensitivity of the optical properties of FAM to these conditions.[49] The reproducibility of these experiments was checked by the carrying out of two to three independent experiments. Selectivity experiments for various ROS and reductants were carried out by the same method.

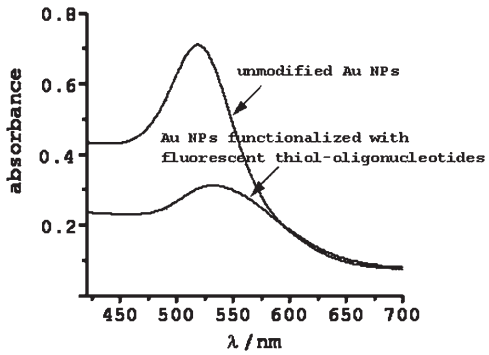

Figure 7. Comparison of UV/Vis spectra of 15 nm diameter Au NPs and of Au NPs functionalized with fluorescent thiol-oligonucleotides in fresh PBS (0.3 M, pH 7.4).

Cell culture and imaging: Peritoneal exudate cells were harvested from peritoneal lavage with use of chilled serum-free RPMI 1640 medium, centrifuged at 1000 rpm for 5 min, and suspended with PBS. The concentration of counted cells was adjusted to 10^5 cells mL^{-1} and samples were placed on the culture plates above glass coverslips. After 3 h of incubation at 37 °C in an atmosphere of 5% CO_2 in a CO_2 incubator, the nonadherent cells were removed by vigorous washing (×2) with warm serum-free medium, and the adherent cells were incubated with 1× probe solutions (0.3 M PBS, pH 7.4) for 30 min at 37 °C. A set of cells was stimulated with PMA (2 ng mL^{-1}) at 37 °C for 1 h. Another set of cells was treated with DMSO (0.1%) for 1 h prior to PMA stimulation. HepG2 cells (human cancerous liver cells) were maintained by protocols provided by the American Type Tissue Culture Collection. Cells were seeded at a density of 10^6 cells mL^{-1} in high-glucose Dulbecco's Modified Eagle's Medium (DMEM, 4.5 g L^{-1} glucose) supplemented with fetal bovine serum (FBS, 10%), $NaHCO_3$ (2 g L^{-1}), and antibiotics (penicillin 100 U mL^{-1}, streptomycin 100 μg mL^{-1}). Cultures were maintained at 37 °C under a humidified atmosphere containing 5% CO_2.

Prior to imaging, the medium was removed. Cell imaging was carried out after washing of cells with PBS to stop the progress of the labeling reaction.

AO, generally regarded as a marker of apoptosis, was used to visualize cellular changes characteristic of apoptosis and to confirm that the cells were viable throughout the imaging experiments. Probe-loaded macrophages and HepG2 were incubated with acridine orange (1 μg mL^{-1}) at 37 °C for 20 min. After washing with ice-cold PBS, the cells were observed under a microscope. Florescent images were acquired on a LSM 510 confocal laser scanning microscope (Carl Zeiss Co., Ltd.) with commonly used Ar^+ laser irradiation at 488 nm.

Cell extracts: Cultured macrophages (RAW 264.7 cells were purchased from the American Type Culture Collection, Manassas) were passaged in cell culture flasks (10^6 cells mL^{-1}) in DMEM. Incubation of a proportion of the macrophage cells with HO• scavenger DMSO (0.1%) for 1 h prior to probe loading resulted in autofluorescence output. Stimulation of another portion of macrophage cells with PMA (2 ng mL^{-1}) at 37 °C for 12 h was then carried out. After incubation with 1× probe solutions for 30 min at 37 °C, all of the cells, harvested by centrifugation in the cold, were washed twice with NaCl solution (0.9%). These cells were again resuspended in a volume of PBS (0.1 M, pH 7.4) equal to that in the

 © 2008 Wiley-VCH Verlag GmbH & Co. KGaA, Weinheim

DMEM medium in which they had been grown, and were then disrupted for 10 min in a VC 130 PB ultrasonic disintegrator (Sonics & Materials Inc.). During sonic disruption, the temperature was maintained below 4 °C with circulating ice water. The broken cell suspension was centrifuged at 4000 rpm for 10 min and the pellet was discarded. Cell supernatant solutions obtained were prepared for average recovery test.

Acknowledgements

The authors gratefully acknowledge the financial support received from the National Basic Research Program of China (973 Program, 2007CB936000), the Program for New Century Excellent Talents in Universities (NCET-04-0651), the National Natural Science Foundation of China (Nos. 20335030, 20575036, and 20475034), and the Important Project of Natural Science Foundation of Shandong Province, China (No. Z2006B09).

[1] K. Hsiao, P. Chapman, S. Nilsen, C. Eckman, Y. Harigaya, S. Younkin, F. S. Yang, G. Cole, *Science* **1996**, *274*, 99–103.
[2] D. C. Malins, N. L. Polissar, S. J. Gunselman, *Proc. Natl. Acad. Sci. USA* **1996**, *93*, 2557–2563.
[3] T. Finkel, N. J. Holbrook, *Nature* **2000**, *408*, 239–247.
[4] C. M. de Lara, M. A. Hill, T. J. Jenner, D. Papworth, P. O'Neill, *Radiat. Res.* **2001**, *155*, 440–448.
[5] E. Cabiscol, J. Tamarit, J. Ros, *Int. Microbiol.* **2000**, *3*, 3–8.
[6] M. Tien, B. A. Svingen, S. D. Aust, *Arch. Biochem. Biophys.* **1982**, *216*, 142–151.
[7] J. J. Briede, T. M. C. M. de Kok, J. G. F. Hogervorst, E. J. C. Moonen, C. L. B. op den Camp, J. C. S. Kleinjans, *Environ. Sci. Technol.* **2005**, *39*, 8420–8426.
[8] J. Zheng, S. R. Springston, J. Weinstein-Lloyd, *Anal. Chem.* **2003**, *75*, 4696–4700.
[9] M. C. Y. Chang, A. Pralle, E. Y. Isacoff, C. J. Chang, *J. Am. Chem. Soc.* **2004**, *126*, 15392–15393.
[10] E. Sasaki, H. Kojima, H. Nishimatsu, Y. Urano, K. Kikuchi, Y. Hirata, T. Nagano, *J. Am. Chem. Soc.* **2005**, *127*, 3684–3685.
[11] K. Setsukinai, Y. Urano, K. Kakinuma, H. J. Majima, T. Nagano, *J. Biol. Chem.* **2003**, *278*, 3170–3175.
[12] K. H. Xu, X. Liu, B. Tang, G. W. Yang, Y. Yang, L. G. An, *Chem. Eur. J.* **2007**, *13*, 1411–1416.
[13] a) T. Karin, O. Stefan, *FEMS Microbiol. Ecol.* **2002**, *40*, 13–20; b) N. Soh, K. Makihara, E. Sakoda, T. Imato, *Chem. Commun.* **2004**, *5*, 496–497.
[14] G. M. Makrigiorgos, J. Baranowska-Kortylewicz, E. Bump, S. K. Sahu, R. M. Berman, A. I. Kassis, *Int. J. Radiat. Biol.* **1993**, *63*, 445–458.
[15] B. Li, P. L. Gutierrez, N. V. Blough, *Anal. Chem.* **1997**, *69*, 4295–4302.
[16] C. P. LeBel, H. Ischiropoulos, S. C. Bondy, *Chem. Res. Toxicol.* **1992**, *5*, 227–231.
[17] K. Setsukinai, Y. Urano, K. Kikuchi, T. Higuchi, T. Nagano, *J. Chem. Soc. Perkin Trans. 2* **2000**, 2453–2457.
[18] S. L. Hempel, G. R. Buettner, Y. Q. O'Malley, D. A. Wessels, D. M. Flaherty, *Free Radical Biol. Med.* **1999**, *27*, 146–159.
[19] Y. Nagasaki, T. Ishii, Y. Sunaga, Y. Watanabe, H. Otsuka, K. Kataoka, *Langmuir* **2004**, *20*, 6396–6400.
[20] A. R. Clapp, I. L. Medintz, J. M. Mauro, B. R. Fisher, M. G. Bawendi, H. Mattoussi, *J. Am. Chem. Soc.* **2004**, *126*, 301–310.
[21] D. M. Willard, L. L. Carillo, J. Jung, A. Van Orden, *Nano Lett.* **2001**, *1*, 469–474.
[22] S. Wang, N. Mamedova, N. A. Kotov, W. Chen, J. Studer, *Nano Lett.* **2002**, *2*, 817–822.
[23] B. Dubertret, M. Calame, A. J. Libchaber, *Nat. Biotechnol.* **2001**, *19*, 365–370.
[24] Y. C. Cao, R. Jin, C. A. Mirkin, *Science* **2002**, *297*, 1536–1540.
[25] C. A. Mirkin, R. L. Letsinger, R. C. Mucic, J. J. Storhoff, *Nature* **1996**, *382*, 607–609.
[26] A. P. Alivisatos, K. P. Johnsson, X. G. Peng, T. E. Wilson, C. J. Loweth, M. P. Bruchez, Jr, P. G. Schultz, *Nature* **1996**, *382*, 609–611.
[27] H. Li, L. J. Rothberg, *Anal. Chem.* **2004**, *76*, 5414–5417.
[28] E. Dulkeith, M. Ringler, T. A. Klar, J. Feldmann, A. Munoz Javier, W. J. Parak, *Nano Lett.* **2005**, *5*, 585–589.
[29] J. Wang, J. Li, A. J. Baca, J. Hu, F. Zhou, W. Yan, D.-W. Pang, *Anal. Chem.* **2003**, *75*, 3941–3945.
[30] L. Authier, C. Grossiord, P. Brossier, B. Limoges, *Anal. Chem.* **2001**, *73*, 4450–4456.
[31] A. C. Mello Filho, M. E. Hoffmann, R. Meneghini, *Biochem. J.* **1984**, *218*, 273–275.
[32] R. Meneghini, M. E. Hoffmann, *Biochim. Biophys. Acta* **1980**, *608*, 167–173.
[33] D. K. Hazra, S. Steenken, *J. Am. Chem. Soc.* **1983**, *105*, 4380–4386.
[34] M. Roessle, E. Zaychikov, L. Denissova, M. Wulff, F. Schotte, M. Hanfland, B. Sclavi, C. Badaut, M. Buckle, H. Heumann, *ESRF NewsLett.* **2000**, *34*, 24–26.
[35] M. Stork, B. S. Gaylord, A. J. Heeger, G. C. Bazan, *Adv. Mater.* **2002**, *14*, 361–366.
[36] J. R. Lakowicz, *Principles of Fluorescence Spectroscopy*, Plenum Press, New York, 2nd ed., **1999**, p. 237.
[37] A. Jorns, M. Tiepge, S. Lenzen, R. Munday, *Free Radical Biol. Med.* **1999**, *26*, 1300–1304.
[38] B. Halliwell, J. M. C. Gutteridge, *Arch. Biochem. Biophys.* **1986**, *246*, 501–514.
[39] P. Sandström, B. Åkerman, *Langmuir* **2004**, *20*, 4182–4186.
[40] L. M. Demers, C. A. Mirkin, R. C. Mucic, R. A. Reynolds III, R. L. Letsinger, R. Elghanian, G. Viswanadham, *Anal. Chem.* **2000**, *72*, 5535–5541.
[41] E. R. Stadtman, *Annu. Rev. Biochem.* **1993**, *62*, 797–821.
[42] J. M. Gutteridge, *Biochem. J.* **1987**, *243*, 709–714.
[43] N. L. Rosi, D. A. Giljohann, C. S. Thaxton, A. K. R. Lytton-Jean, M. S. Han, C. A. Mirkin, *Science* **2006**, *312*, 1027–1030.
[44] M. C. Raff, *Science* **1994**, *264*, 668–669.
[45] G. Frens, *Nat. Phys. Sci.* **1973**, *241*, 20–22.
[46] S. J. Chen, H. T. Chang, *Anal. Chem.* **2004**, *76*, 3727–3734.
[47] R. Elghanian, J. J. Storhoff, R. C. Mucic, R. L. Letsinger, C. A. Mirkin, *Science* **1997**, *277*, 1078–1080.
[48] J. J. Storhoff, R. Elghanian, R. C. Mucic, C. A. Mirkin, R. L. Letsinger, *J. Am. Chem. Soc.* **1998**, *120*, 1959–1964.
[49] Z. Zhao, T. Shen, H. Xu, *Spectrochim. Acta* **1989**, *45*, 1113–1116.

Received: March 24, 2007
Revised: May 22, 2007
Published online: October 30, 2007

 © 2008 Wiley-VCH Verlag GmbH & Co. KGaA, Weinheim